

UK/TP 97-10  
hep-ph/9707385  
July 1997

## Rho-Omega Mixing and the Pion Form Factor in the Time-like Region

S. Gardner and H.B. O'Connell  
*Department of Physics and Astronomy, University of Kentucky,  
Lexington, KY 40506-0055*

### Abstract

We determine the magnitude, phase, and  $s$ -dependence of  $\rho$ - $\omega$  “mixing” in the pion form factor in the time-like region through fits to  $e^+e^- \rightarrow \pi^+\pi^-$  data. The associated systematic errors in these quantities, arising from the functional form used to fit the  $\rho$  resonance, are small. The systematic errors in the  $\rho$  mass and width, however, are larger than previously estimated.

## I. INTRODUCTION

The pion form factor  $F_\pi(s)$  in the time-like region is extracted from cross section measurements of  $e^+e^- \rightarrow \pi^+\pi^-$ , namely,

$$\sigma(s) = \sigma_{\text{em}}(s)|F_\pi(s)|^2, \quad (1)$$

where  $\sigma_{\text{em}}(s)$  is the cross section to produce a structureless  $\pi^+\pi^-$  pair and  $s$  is the usual Mandelstam variable. The isovector  $\rho$  resonance dominates the cross section for  $\sqrt{s}$  ranging from 600 to 900 MeV, though isospin violation allows the isoscalar  $\omega$  resonance to contribute as well. We wish to extract the rho-omega “mixing” matrix element  $\tilde{\Pi}_{\rho\omega}(s)$ , which to leading order in isospin violation is given by

$$F_\pi(s) = F_\rho(s) \left( 1 + \frac{1}{3} \left( \frac{\tilde{\Pi}_{\rho\omega}(s)}{s - m_\omega^2 + im_\omega\Gamma_\omega} \right) \right), \quad (2)$$

from data. Note that  $F_\rho(s)$  is the pion form factor in the absence of isospin violation.  $F_\rho(s)$  is subject only to general theoretical constraints; it is our purpose to determine how its non-uniqueness impacts the extraction of  $\tilde{\Pi}_{\rho\omega}$ . Moreover, the  $\rho$  mass and width are themselves sensitive to the choice of  $F_\rho(s)$  [1–3], and we wish to determine the systematic error in these quantities as well.

Maltman *et al.* have discussed the separation of  $\tilde{\Pi}_{\rho\omega}(s)$  into two contributions: one from the direct coupling of  $\omega \rightarrow 2\pi$  and the other from mixing,  $\omega \rightarrow \rho \rightarrow 2\pi$  [6,4,5]. Such a separation is model dependent, and we shall not pursue it further. Rather, we wish to determine the constraint  $e^+e^- \rightarrow \pi^+\pi^-$  data places on the sum of these contributions; we term  $\tilde{\Pi}_{\rho\omega}(s)$  the effective mixing matrix element.  $\tilde{\Pi}_{\rho\omega}(s)$  is usually assumed to be both real and approximately  $s$ -independent [7]; we wish also to test these assumptions in the context of  $e^+e^- \rightarrow \pi^+\pi^-$  data. An explicit  $s$ -dependence in  $\tilde{\Pi}_{\rho\omega}(s)$  emerges as a consequence of the inclusion of a non-resonant contribution to  $\omega \rightarrow 2\pi$  [4,5]; thus, the  $s$ -dependence of the effective mixing amplitude in the resonance region may partially constrain the role of this contribution.

Previous determinations of  $\tilde{\Pi}_{\rho\omega}(s)$  have used either the empirical  $\omega \rightarrow 2\pi$  branching ratio [9,10] or  $e^+e^- \rightarrow \pi^+\pi^-$  data [6,11,4,5]. We prefer the latter method for several reasons. Information on the phase and  $s$ -dependence of  $\tilde{\Pi}_{\rho\omega}(s)$  is not accessible from the  $\omega \rightarrow 2\pi$  branching ratio. Moreover, the determined  $\rho$ - $\omega$  mixing matrix element then explicitly depends on the relatively poorly known  $\rho$  resonance parameters.

Our work differs from earlier analyses in that we enumerate a variety of forms for  $F_\rho(s)$  which satisfy the known theoretical constraints. We extract the magnitude, phase, and  $s$ -dependence of the effective  $\rho$ - $\omega$  mixing matrix element  $\tilde{\Pi}_{\rho\omega}(s)$  from  $e^+e^- \rightarrow \pi^+\pi^-$  data and study the systematic error in the above parameters resulting from the choice of  $F_\rho(s)$ . We have also studied the systematic errors in the  $\rho$  parameter extraction and find them to be much larger than previously reported.

To extract  $\tilde{\Pi}_{\rho\omega}(s)$  from  $e^+e^- \rightarrow \pi^+\pi^-$  data we naturally wish to use the best data set available. The most recent data for the pion form factor in the time-like region is due to Barkov *et al.* [12]. They report  $m_\rho = 775.9 \pm 0.8 \pm 0.8$  MeV and  $\Gamma_\rho = 150.5 \pm 1.6 \pm 2.5$  MeV, where the errors respectively refer to the error arising from the statistical and systematic

uncertainties in the experimental data and to the systematic error resulting from the form chosen for the pion form factor [12]. The Barkov *et al.* value for the  $\rho$  mass contributes some 40% of the  $\chi^2$  in the Particle Data Group's 1994 world average for this quantity [13]. In the 1996 compilation, the Particle Data Group rule the Barkov *et al.*  $\rho$  mass “probably wrong” on statistical grounds and exclude the Barkov *et al.* values from the world averages for the  $\rho$  mass and width [14,1]. The only determination of the  $\rho$  mass currently included in the Particle Data Group world average based, at least in part, on time-like pion form factor data is that of Heyn and Lang [15]. We apply our analysis to both the data included in Barkov *et al.* [12,16] and to the time-like region data included in Heyn and Lang [15,17], to ascertain whether any systematic differences exist between the data sets.

The  $\rho$  resonance is relatively broad, so that the reported resonance parameters are numerically sensitive to the convention under which the mass and width are defined. The appearance of a resonance is associated with a complex pole at  $s = s_p$  in the elastic scattering amplitude, and this complex pole can be used to define the resonance's mass and width [18]. The separation of  $s_p$  into a mass and width is not unique, however, for both the real and imaginary parts of  $s_p$  appear in any physical process [19]. Thus, whether one defines  $s_p \equiv m^2 - im\Gamma$ , so that  $m = \sqrt{\text{Re } s_p}$ , or  $\sqrt{s_p} \equiv \tilde{m} - i\tilde{\Gamma}/2$ , so that  $\tilde{m} = \text{Re}\sqrt{s_p}$ , is a matter of convention. We will present results for the  $\rho$  mass and width under both conventions.

## II. THE PION FORM FACTOR AND $\rho$ - $\omega$ “MIXING”

Only general theoretical constraints guide the construction of the pion form factor in the time-like region. Charge conservation requires the form factor to be unity at  $s = 0$ :

$$F_\pi(0) = 1 . \quad (3)$$

Moreover, it should be an analytic function in the complex  $s$  plane, with a branch cut along the real axis beginning at the two-pion threshold,  $s = 4m_\pi^2$ . Finally, time-reversal invariance and the unitarity of the  $S$  matrix requires that the phase of the form factor be that of  $l = 1$ ,  $I = 1$   $\pi$ - $\pi$  scattering [20]. This last emerges as  $\pi$ - $\pi$  scattering in the relevant channel is very nearly elastic from threshold through  $s \approx (m_\pi + m_\omega)^2$  [21,15]. In this region of  $s$ , then, the form factor is related to the  $l = 1$ ,  $I = 1$  phase shift,  $\delta_1^1$ , via [22]

$$F_\pi(s) = e^{2i\delta_1^1} F_\pi^*(s) \quad (4)$$

so that

$$\tan \delta_1^1(s) = \frac{\text{Im } F_\pi(s)}{\text{Re } F_\pi(s)} . \quad (5)$$

The above is a special case of what is sometimes called the Fermi-Watson-Aidzu phase theorem [22,23].

In the resonance region the phase and analyticity constraints can be realized via the Breit-Wigner form

$$\lim_{s \rightarrow m_\rho^2} F_\pi(s) = -\frac{m_\rho^2(1 + \varepsilon)}{s - m_\rho^2 + im_\rho\Gamma_\rho} , \quad (6)$$

where  $\varepsilon$  is a real constant. The complex pole  $s_p$  associated with the appearance of the resonance is given by  $s_p \equiv m_\rho^2 - im_\rho\Gamma_\rho$ . We have adopted the  $\sqrt{\text{Re } s_p}$  convention for the  $\rho$  mass. Alternatively, one could have written  $\sqrt{s_p} \equiv \tilde{m}_\rho - i\tilde{\Gamma}_\rho/2$ , so that  $\tilde{m} = \text{Re}\sqrt{s_p}$ , but this is merely a matter of convention. Note that the  $m$  and  $\tilde{m} = \text{Re}\sqrt{s_p}$  prescriptions are related via [15]

$$\tilde{m} = \left( \frac{m^2 + \sqrt{m^4 + m^2\Gamma^2}}{2} \right)^{1/2}, \quad \tilde{\Gamma} = \frac{m}{\tilde{m}}\Gamma. \quad (7)$$

The Breit-Wigner form Eq. (6) only satisfies the phase constraint as  $s \rightarrow m_\rho^2$ , so that a more general form for the pion form factor, suitable for all  $s$ , is needed. Generalizations satisfying the enumerated constraints have been constructed by various authors [24,15,25]; we will follow the work of Gounaris and Sakurai [24] and of Heyn and Lang [15] in what follows. We include  $\rho$ - $\omega$  mixing as per Eq. (2), so that our enumerated constraints are brought to bear on the form of  $F_\rho(s)$  alone, for the violations of the above constraints due to isospin breaking are small.

Gounaris and Sakurai consider a  $F_\rho(s)$  of the form  $f(0)/f(s)$  with  $f(s)$  such that

$$f(s) = (k^3/\sqrt{s}) \cot \delta_1^1 - i(k^3/\sqrt{s}), \quad (8)$$

where  $f(0)$  is real. Note that both the normalization and phase constraints are manifest in such a construction. The  $\delta_1^1$  phase shift is parametrized via a generalized effective-range formula of Chew-Mandelstam type [26], with two free parameters,  $a'$  and  $b'$ ,

$$(k^3/\sqrt{s}) \cot \delta_1^1 = a' + b'k^2 + k^2h(s), \quad (9)$$

where  $k$  and  $h(s)$  are chosen to be

$$\begin{aligned} k &= (s/4 - m_\pi^2)^{1/2}, h(s) = \frac{2k}{\pi\sqrt{s}} \log \left( \frac{\sqrt{s} + 2k}{2m_\pi} \right); \quad s \geq 4m_\pi^2 \\ k &= i(m_\pi^2 - s/4)^{1/2}, h(s) = \frac{2ki}{\pi\sqrt{s}} \text{arccot} \left( \frac{s}{4m_\pi^2 - s} \right)^{1/2}; \quad 0 \leq s < 4m_\pi^2. \end{aligned} \quad (10)$$

In this manner the required analytic structure is imposed as well. The parameters  $a'$  and  $b'$  can be replaced by functions of  $m_\rho$  and  $\Gamma_\rho$  by noting the resonance conditions  $\cot \delta_1^1(m_\rho^2) = 0$  and  $\delta_1^{1'}(m_\rho^2) = 1/(m_\rho\Gamma_\rho)$ , so that the resulting form factor is of the form [24]

$$F_\rho^{\text{GS}}(s) = \frac{-(m_\rho^2 + dm_\rho\Gamma_\rho)}{s - m_\rho^2 - \Gamma_\rho(m_\rho^2/k_\rho^3)[k^2(h - h_\rho) - (s - m_\rho^2)k_\rho^2h'] + im_\rho\Gamma_\rho(s)}, \quad (11)$$

where

$$k_\rho = k(m_\rho^2), \quad h_\rho = h(m_\rho^2), \quad \Gamma_\rho(s) = \Gamma_\rho \left( \frac{k}{k_\rho} \right)^3 \frac{m_\rho}{\sqrt{s}}, \quad (12)$$

and  $d$  is fixed in terms of  $m_\rho$  and  $m_\pi$ ,

$$d = \frac{3m_\pi^2}{\pi k_\rho^2} \log \left( \frac{m_\rho + 2k_\rho}{2m_\pi} \right) + \frac{m_\rho}{2\pi k_\rho} - \frac{m_\rho m_\pi^2}{\pi k_\rho^3} . \quad (13)$$

Note that the Breit-Wigner form, Eq. (6), is recovered as  $s \rightarrow m_\rho^2$ . It turns out that the two-parameter fit of Eq. (11) does not suffice to fit the pion form factor data in the  $\rho$  resonance region, and a modification of  $F_\rho^{\text{GS}}(s)$  to include a multiplicative real function of  $s$ , constrained by only the normalization condition, is phenomenologically necessary.

It is critical to note that the adoption of an  $s$ -dependent width,  $\Gamma(s)$ , predicated by the phase constraint of Eq. (5), implies that  $s = m_\rho^2 - im_\rho\Gamma_\rho$  no longer determines the position of the complex pole  $s_p$  [27]. Rather, if one were to determine the mass and width from  $s_p \equiv \bar{m}_\rho^2 - i\bar{m}_\rho\bar{\Gamma}_\rho$ , where  $f(s_\rho) = 0$ , then for  $s = \bar{m}_\rho^2$  the phase shift would *not* be  $\pi/2$ , and the resultant form factor near  $s = \bar{m}_\rho^2$  would *not* be of Breit-Wigner form. We prefer, then, to determine the resonance parameters by comparing  $f(s)$  to  $s - m_\rho^2 - im_\rho\Gamma_\rho$  at the  $s$  in the physical region where the real part of  $f(s)$  vanishes. The resonance condition  $\cot \delta = \pi/2$  is thus satisfied as  $s \rightarrow m_\rho^2$ . Our procedure is consistent with that of Ref. [24].

Heyn and Lang write  $F_\rho(s)$  as

$$F_\rho(s) = \Omega(s)F_{\text{red}}(s) , \quad (14)$$

where for  $0 \leq s \lesssim (m_\omega + m_\pi)^2$ ,  $F_{\text{red}}(s)$  is purely real and can be approximated by a cubic polynomial [15],

$$F_{\text{red}}(s) = 1 + \beta_1 s + \beta_2 s^2 + \beta_3 s^3 . \quad (15)$$

All phase information is contained in the Omnès function  $\Omega(s)$  [28], which is chosen to be

$$\Omega(s) = \frac{c + m_\pi^2 g(0)}{\tilde{s}_p} \frac{\tilde{s}_p - s}{as^2 + bs + c - (s - 4m_\pi^2)g(s)/4} . \quad (16)$$

Modulo the  $(\tilde{s}_p - s)/\tilde{s}_p$  factor,  $\Omega(s)$  also has a  $f(0)/f(s)$  structure, where now

$$f(s) = as^2 + bs + c - (s - 4m_\pi^2)g(s)/4 \quad (17)$$

and  $g(s)$  is determined by the one-pion-loop diagrams in the  $\rho$  self-energy [29–31],

$$\begin{aligned} g(s) &= -\frac{1}{\pi} u \log \frac{1+u}{1-u} + iu , u = \sqrt{1 - 4m_\pi^2/s} , s \geq 4m_\pi^2 \\ &= -\frac{2}{\pi} u \arctan \frac{1}{u} , u = \sqrt{4m_\pi^2/s - 1} , 0 \leq s \leq 4m_\pi^2 \\ &= -\frac{1}{\pi} u \log \frac{u+1}{u-1} , u = \sqrt{1 - 4m_\pi^2/s} , s < 0 \\ g(0) &= -2/\pi . \end{aligned} \quad (18)$$

The  $\rho$  resonance is associated with a zero of  $f(s)$  in the complex plane for  $s > 4m_\pi^2$ , yet  $f(s)$  also vanishes on the negative real axis when  $s = \tilde{s}_p$ , by definition. This zero simulates the left-hand cut in the  $N/D$  construction of the amplitude [32] and physically corresponds to a bound state [22]. The  $(\tilde{s}_p - s)/\tilde{s}_p$  factor in  $\Omega(s)$  removes this singularity while preserving the normalization constraint. The singularity structure of  $\Omega(s)$  occurs in  $F_{\text{GS}}(s)$  as well;

the zero there, though, is at such large negative  $s$  that the inclusion of a  $(\tilde{s}_p - s)/\tilde{s}_p$  factor would be of no phenomenological impact [24]. Two parameters are needed to describe the left-hand cut. The third free parameter in Eq. (17) functions as a CDD parameter; the  $N/D$  solution of the partial-wave amplitude dispersion relation does not uniquely follow from the information input on the left-hand cut [33,22].

Once  $a$ ,  $b$ , and  $c$  are determined from a fit to data, the  $\rho$  resonance parameters can also be determined. As discussed earlier in the case of the Gounaris and Sakurai form factor [24], Eq. (11), we determine the resonance parameters by comparing  $f(s)$  to  $s - m_\rho^2 - im_\rho\Gamma_\rho$  at the  $s$  in the physical region where the real part of  $f(s)$  vanishes. This has the effect of requiring that  $f(s)$  be of Breit-Wigner form as  $s \rightarrow m_\rho^2$ . Consequently,  $m_\rho$  is determined by  $\text{Re}\{f(m_\rho^2)\} = 0$  and  $\Gamma_\rho$  is determined by  $\text{Im}\{f(m_\rho^2)\} = -m_\rho\Gamma_\rho$  [15].

The structure chosen for  $f(s)$  in Eq. (17) is formally consistent with the phase constraint resulting from unitarity and time-reversal invariance, yet the constraint may not be numerically well-satisfied, as the parameters are fit to the time-like pion form factor data. We can, however, require that the parameters in  $f(s)$  reproduce the empirical  $l = 1$ ,  $I = 1$   $\pi$ - $\pi$  scattering length  $a_1^1$  to gauge whether the results we extract for the  $\rho$  parameters and  $\tilde{\Pi}_{\rho\omega}$  are sensitive to this additional constraint. We define  $a_1^1$  as

$$\frac{1}{a_1^1} = \lim_{s \rightarrow 4m_\pi^2} k^3 \cot \delta_1^1, \quad (19)$$

where empirically  $a_1^1 = (0.038 \pm 0.002) m_\pi^{-3}$  [34]. Note that  $1/a_1^1$  is equal to  $2m_\pi a'$  in the Gounaris and Sakurai model, Eq. (9), and is equal to  $(16m_\pi^4 a + 4m_\pi^2 b + c)m_\pi$  in the Heyn-Lang model, Eq. (16).

The pion form factor we fit to data is

$$F_\pi(s) = \Omega(s)F_{\text{red}}(s) \left[ 1 + \frac{1}{3} \frac{\tilde{\Pi}_{\rho\omega}(s)}{s - m_\omega^2 + im_\omega\Gamma_\omega} \right]. \quad (20)$$

We work to leading order in isospin violation, and we adopt the SU(3) value of 1/3 for the ratio of the electromagnetic coupling of the  $\omega$  to that of the  $\rho$ . Note that  $F_{\text{red}}(s)$  is given by Eq. (15) and  $\Omega(s)$  by Eq. (16), though we will also replace  $\Omega(s)$  by  $F_{\text{GS}}(s)$ , Eq. (11), and by an Omnès function modified to resemble  $F_{\text{GS}}(s)$ ,

$$\Omega_{\text{GS}}(s) = \frac{c + m_\pi^2 g(0)}{bs + c - (s - 4m_\pi^2)g(s)/4}. \quad (21)$$

We thus test the sensitivity of the fit to the specific manner in which the phase constraint is realized. Rather than Eq. (20), Barkov *et al.* [12] adopt a pion form factor such that

$$F_\pi(s) = F_\rho^{\text{GS}}(s) \frac{(1 + \alpha_\omega F_\omega^{\text{GS}}(s) + \alpha_{\rho'} F_{\rho'}^{\text{GS}}(s) + \alpha_{\rho''} F_{\rho''}^{\text{GS}}(s))}{1 + \alpha_\omega + \alpha_{\rho'} + \alpha_{\rho''}}, \quad (22)$$

where  $\alpha_\omega$ ,  $\alpha_{\rho'}$ , and  $\alpha_{\rho''}$  are real constants, to be determined from a fit to data, and  $F_V^{\text{GS}}(s)$ , with  $V$  a vector meson, is determined by Eqs. (11,12,13) with  $m_\rho$ ,  $\Gamma_\rho$  replaced by  $m_V$ ,  $\Gamma_V$ .  $F_V^{\text{GS}}(s)$  is complex in the region of  $s$  we consider, so that Eq. (22) would seem to violate the phase constraint of Eq. (5). We fit Eq. (22) as well to the time-like pion form factor data,

and we will examine the above issue through direct comparison with the  $l = 1$ ,  $I = 1$  phase shifts.

If the inelastic contributions to  $\pi$ - $\pi$  scattering in the  $s$  region of interest are generated by isospin violation only, the solution of the Muskhelishvili-Omnès integral equation [28] with inelastic unitarity suggests that the effective  $\rho$ - $\omega$  mixing matrix element,  $\tilde{\Pi}_{\rho\omega}(s)$ , is real [7]. It is also thought to be weakly  $s$ -dependent [7]. Thus, unless otherwise stated, we make the replacement  $\tilde{\Pi}_{\rho\omega}(s) = \tilde{\Pi}_{\rho\omega}(m_\omega^2)$ . We can, however, also test these assumptions by replacing  $\tilde{\Pi}_{\rho\omega}(s)$  with

$$\tilde{\Pi}_{\rho\omega}(s) \equiv \tilde{\Pi}_{\rho\omega}^{\text{R}}(m_\omega^2) + i\text{Im} \tilde{\Pi}_{\rho\omega}^{\text{I}}(m_\omega^2) \quad (23)$$

or with

$$\tilde{\Pi}_{\rho\omega}(s) = \tilde{\Pi}_{\rho\omega}(m_\omega^2) + (s - m_\omega^2)\tilde{\Pi}'_{\rho\omega}(m_\omega^2), \quad (24)$$

where it is natural to expand the  $s$ -dependence of the effective mixing matrix element about  $s = m_\omega^2$ . In this manner we can test whether the value of  $\text{Re}\{\tilde{\Pi}_{\rho\omega}(m_\omega^2)\}$  is sensitive to the matrix element's possible  $s$  dependence or phase.

### III. RESULTS

We optimize the fit parameters using MINUIT [35]. The parameters can be highly correlated, so that we compute the correlation coefficients and final errors with a double precision FORTRAN code using standard techniques [36]. We fit data from threshold,  $\sqrt{s} = 2m_\pi \sim 280$  MeV, through  $\sqrt{s} \approx m_\omega + m_\pi = 923$  MeV, as this is the region in which the empirical  $l = 1$ ,  $\pi = 1$  phase shift is essentially elastic [21]. Our data set consists of the 82 points in this energy range included in the analysis of Barkov *et al.* [12,16]. The following fits are based on Eq. (20) — the forms chosen for  $\Omega(s)$ ,  $F_{\text{red}}(s)$ , and  $\tilde{\Pi}_{\rho\omega}(s)$  in each fit are indicated in Table I. For fits B and C above, a fit of the type indicated by A' and A<sup>I</sup> has been performed as well, so that B' and B<sup>I</sup>, *e.g.*, indicate B-type fits in which  $\tilde{\Pi}_{\rho\omega}(s)$  has been replaced by Eq. (24) and Eq. (23), respectively. Note that in fit B the parameter  $c$  is fixed so that the model reproduces the empirical scattering length,  $a_1^1 = (0.038 \pm 0.002) m_\pi^{-3}$  [34], as per Eq. (19). For definiteness, note that we use  $m_\pi = 139.57$  MeV,  $m_\omega = 781.94$  MeV, and  $\Gamma_\omega = 8.43$  MeV [1] in all fits. The results are given in Tables II and III. The given parameter errors arise from the  $\chi^2$  optimization of the fit to data, whose errors include both statistical and experimental systematic uncertainties. Specifically, the parameter errors are given by the square root of the diagonal elements of the inverse of the curvature matrix [36]. The parameters are correlated, so that the errors in the “Output” of Tables II and III are generated using the full error matrix. All the parametrized forms are able to fit the data exceedingly well —  $\chi^2/\text{dof} \approx 1$  in all cases. Fits A and B, along with the Heyn-Lang A-type fit [15] to the 1978 world data [17], are plotted as a function of the pion-pair invariant mass  $q$ ,  $q \equiv \sqrt{s}$ , with the data [16] included in the compilation of Ref. [12] in Fig. 1. The shapes of A and B are very similar in the resonance region but are visibly different at small  $q$  as fit B is constrained to reproduce the empirical  $a_1^1$  scattering length. The scattering length extracted from fit A is nearly a factor of 2 larger than the empirical value; later we will

explicitly compare the phase of the fits we generate with the measured  $l = 1$ ,  $I = 1$   $\pi$ - $\pi$  phase shift in the  $s$  range of interest.

The effective  $\rho$ - $\omega$  mixing matrix element  $\tilde{\Pi}_{\rho\omega}(m_\omega^2)$  is remarkably insensitive to the  $\rho$  parametrization chosen; the value we find is  $-3500 \pm 300$  MeV<sup>2</sup>. This insensitivity is significant, for the  $\rho$  mass varies by some 10 MeV over the same set of the parametrizations. It is likely the consequence of the narrow  $\omega$  width; in particular  $\Gamma_\rho/\Gamma_\omega \sim 20$  [1]. The  $s$ -dependence and phase of  $\tilde{\Pi}_{\rho\omega}(s)$ , as per Eq. (24) and Eq. (23), are also relatively insensitive to the  $\rho$  parametrization; this is shown in Tables II and III. We conclude that  $\tilde{\Pi}'_{\rho\omega}$  and  $\tilde{\Pi}^I_{\rho\omega}(m_\omega^2)$  are  $0.03 \pm 0.04$  and  $-300 \pm 300$  MeV<sup>2</sup>, respectively. The errors are such that both  $\tilde{\Pi}'_{\rho\omega}$  and  $\tilde{\Pi}^I_{\rho\omega}(m_\omega^2)$  are consistent with zero. This is consistent with the conclusions of Costa de Beauregard *et al.* [7], and thus their implicit assumptions would seem to be justified in the resonance region. Note that the value of  $\text{Re}\{\tilde{\Pi}_{\rho\omega}(m_\omega^2)\}$  continues to be  $-3500 \pm 300$  MeV<sup>2</sup> in the presence of  $s$ -dependent or imaginary contributions to  $\tilde{\Pi}_{\rho\omega}(s)$ ; this is plausible as these corrections are themselves consistent with zero. Moreover, the inferred  $\rho$  parameters are insensitive to the inclusion of these effects as well.

We also consider fits based on the form used by Barkov *et al.*, Eq. (22). Fit E uses Particle Data Group values for the higher  $\rho$  resonances [1]; fit F uses the values adopted by Barkov *et al.* [12]. These parameters, along with the results of fits D, E, and F, are given in Table IV. The values of  $\tilde{\Pi}_{\rho\omega}(m_\omega^2)$  for fits E and F are determined from the fit to Eq. (22) via the relation

$$\tilde{\Pi}_{\rho\omega}(m_\omega^2) = \frac{-3(m_\omega^2 + d_\omega m_\omega \Gamma_\omega) \alpha_\omega}{1 + \alpha_\omega + \alpha_{\rho'} + \alpha_{\rho''}}, \quad (25)$$

where  $d_\omega$  follows from Eq. (13) with  $m_\rho, \Gamma_\rho \rightarrow m_\omega, \Gamma_\omega$ . The final error in the  $\tilde{\Pi}_{\rho\omega}(m_\omega^2)$  of fits E and F is determined by the full error matrix from the fit with Eq. (22). The form of Eq. (22) is quite different from that of Eq. (20), yet the values of  $\tilde{\Pi}_{\rho\omega}(m_\omega^2)$  are comparable, *cf.*  $-3600 \pm 300$  MeV<sup>2</sup> with  $-3500 \pm 300$  MeV<sup>2</sup> from fits A–D. We favor the latter value as the  $\rho'$  and  $\rho''$  contributions in Eq. (22) serve as sources of phase beyond that generated by  $F_\rho(s)$ . We will examine whether such a construction is explicitly at odds with  $\pi$ - $\pi$  scattering data. Note, however, that the scattering lengths extracted from fits D–F are reasonably close to the empirical value, though as  $s$  approaches threshold the impact of the imaginary part of the  $\rho'$  and  $\rho''$  contributions is minimized.

The strength of  $\rho$ - $\omega$  mixing is commonly extracted from the  $\omega \rightarrow 2\pi$  branching ratio [9,10], so that it is useful to reexamine this analysis and compare it with the current results. The physical  $|\omega\rangle$  and  $|\rho^0\rangle$  are related to the isospin-pure states  $|\omega_I\rangle$  and  $|\rho_I^0\rangle$  via the transformation [4]

$$\begin{pmatrix} |\rho_0\rangle \\ |\omega\rangle \end{pmatrix} = \begin{pmatrix} 1 & -\varepsilon_1 \\ \varepsilon_2 & 1 \end{pmatrix} \begin{pmatrix} |\rho_I^0\rangle \\ |\omega_I\rangle \end{pmatrix} \quad (26)$$

to leading order in isospin violation. Assuming that the vector mesons couple to conserved currents,  $\varepsilon_1$  and  $\varepsilon_2$  are determined by requiring that the physical mixed propagator  $D_{\rho\omega}^{\mu\nu}(s)$  has no poles, so that  $\varepsilon_1 = \Pi_{\rho\omega}(m_\omega^2 - im_\omega\Gamma_\omega)/(m_\omega^2 - m_\rho^2 + i(m_\rho\Gamma_\rho - m_\omega\Gamma_\omega))$  and  $\varepsilon_2 = \Pi_{\rho\omega}(m_\rho^2 - im_\rho\Gamma_\rho)/(m_\omega^2 - m_\rho^2 + i(m_\rho\Gamma_\rho - m_\omega\Gamma_\omega))$ . Then



$$\langle \pi^+ \pi^- | \omega \rangle = \langle \pi^+ \pi^- | \omega_I \rangle + \frac{\Pi_{\rho\omega}(m_\rho^2 - im_\rho\Gamma_\rho)}{m_\omega^2 - m_\rho^2 + i(m_\rho\Gamma_\rho - m_\omega\Gamma_\omega)} \langle \pi^+ \pi^- | \rho_I^0 \rangle \quad (27)$$

$$\equiv \frac{\tilde{\Pi}_{\rho\omega}(m_\omega^2)}{m_\omega^2 - m_\rho^2 + i(m_\rho\Gamma_\rho - m_\omega\Gamma_\omega)} \langle \pi^+ \pi^- | \rho_I^0 \rangle, \quad (28)$$

so that

$$\frac{\Gamma(\omega \rightarrow \pi^+ \pi^-)}{\Gamma(\rho \rightarrow \pi^+ \pi^-)} = \frac{p_\omega^3 m_\rho^2}{p_\rho^3 m_\omega^2} \left( \frac{|\tilde{\Pi}_{\rho\omega}(m_\omega^2)|^2}{(m_\rho^2 - m_\omega^2)^2 + (m_\rho\Gamma_\rho - m_\omega\Gamma_\omega)^2} \right), \quad (29)$$

where the overall  $p_\omega^3 m_\rho^2 / (p_\rho^3 m_\omega^2)$  factor arises from treating  $\langle \pi^+ \pi^- | \rho_I^0 \rangle$ , *e.g.*, as the  $g_{\rho\pi\pi}$  coupling as per Ref. [29]. We assume that  $\Gamma(\rho \rightarrow \pi^+ \pi^-) = \Gamma_\rho$  and that  $\langle \pi^+ \pi^- | \rho \rangle = \langle \pi^+ \pi^- | \rho_I \rangle$ , as corrections to the latter are of nonleading order in isospin violation. Using the Particle Data Group values for the  $\omega \rightarrow 2\pi$  branching ratio,  $2.21 \pm .30\%$ , and for the  $\rho$  and  $\omega$  resonance parameters [1] yields a central value of  $|\tilde{\Pi}_{\rho\omega}| = 3860 \text{ MeV}^2$ , whereas using the Barkov *et al.*  $\omega \rightarrow 2\pi$  branching ratio,  $2.3 \pm 0.4 \pm 0.2\%$ , and  $m_\rho = 775.9 \text{ MeV}$  and  $\Gamma_\rho = 150.5 \text{ MeV}$  as per their analysis [12] yields  $|\tilde{\Pi}_{\rho\omega}| = 3950 \text{ MeV}^2$  [37]. Note that their  $\omega \rightarrow 2\pi$  branching ratio is itself extracted from Eq. (22), though this and the PDG value use the estimated leptonic widths  $\Gamma(\rho \rightarrow e^+ e^-)$  and  $\Gamma(\omega \rightarrow e^+ e^-)$  to infer the ratio of the  $\omega$  to  $\rho$  electromagnetic couplings, rather than adopt the  $SU(3)$  value of  $1/3$  as we do [31]. This explains why the above results are of slightly larger magnitude than the result for  $\tilde{\Pi}_{\rho\omega}$ ,  $-3500 \pm 300 \text{ MeV}^2$ , which emerges from the direct analysis of  $e^+ e^- \rightarrow \pi^+ \pi^-$  data in the time-like region. We prefer the latter analysis, however, for  $\tilde{\Pi}_{\rho\omega}$  is accessed directly and is not subject to uncertainties in the  $\rho$  parametrization and its associated parameters.

As the value of the  $\rho$  mass extracted by the analysis of Barkov *et al.* has been called into question on statistical grounds [14,1], it is prudent to examine the sensitivity of our results to the chosen data set. Previously we have used the 82 data points with  $\sqrt{s} \lesssim 923 \text{ MeV}$  compiled by Barkov *et al.* and used in their analysis [16]. We have repeated fits A–C on the 40 points of the 1978 world data [17] used by HL [15] and on the 61 data points from the OLYA and CMD detectors reported by Barkov *et al.* [12] in the  $s$  region of interest. Our results are shown in Table V. Note that the fit B errors refer to the errors generated by uncertainties in the data and by the error in the scattering length, respectively. We see that the parameters obtained for a given fit are consistent within errors for the three data sets. Note, moreover, that the striking insensitivity of  $\tilde{\Pi}_{\rho\omega}(m_\omega^2)$  to the  $\rho$  parametrization is manifest in all the data sets considered.

The fits we have considered support a wide range of  $\rho$  masses and widths.  $m_\rho$ , for example, ranges from 763.1 to 774.2 MeV, whereas  $\Gamma_\rho$  ranges from 144.0 to 157.0 MeV. The median values are 768.7 and 150.7 MeV respectively, remarkably close to the values reported by the Particle Data Group [1]. It is worth noting that the two-parameter Gounaris-Sakurai form, realized as either fit C, D, E, or F, recalling Eqs. (20,22) and Tables I and IV), consistently returns a value of 774 MeV, though fits D, E, and F all possess  $\rho$  widths some 10 MeV smaller than that of fit C. Fits C and D only really differ in the manner they parametrize the  $s$ -dependence of the phase of the pion form factor, *cf.*  $h(s)$ , Eqs. (10,9), of fit C with  $g(s)$ , Eqs. (18,17), of fit D.

The phase constraint can still be used to discriminate between the fits, for the phase of the form factor must be numerically that of  $l = 1$ ,  $I = 1$  scattering, if the latter is elastic.

We explore this issue in Fig. 2, in which the phase of fits A, C, E, and F are shown as a function of the invariant mass  $q$ ,  $q \equiv \sqrt{s}$ , and compared with data [21]. In plotting the  $l = 1$ ,  $I = 1$  phase shifts, we have adopted the energy-independent analysis of Hyams *et al.* [21] and the energy-dependent analysis of Protopescu *et al.* [21]. The above analyses must assume isospin symmetry to separate the  $\delta_l^I$  phase shifts, so that we omit the  $\omega$  contribution from our plots of the phase of  $F_\pi(s)$  determined from fits to the time-like pion form factor data. We have omitted fit D as its phase is essentially identical to fit C, which is shown. Fits C and D differ in how they parametrize the  $s$ -dependence of the phase of the pion form factor, yet this has no impact on the extracted  $\pi$ - $\pi$  phase shift. The  $\rho$  widths for fits C and D do differ by some 10 MeV, but this is of no consequence for the accompanying phase shifts, as  $\tan^{-1}(\text{Im}F_\pi/\text{Re}F_\pi) \rightarrow \pi/2$  as  $s \rightarrow m_\rho^2$ . Fits B–F are reasonably consistent with data, though to judge this in detail we have computed the  $\chi^2$  to the  $\pi$ - $\pi$  scattering data for the fits shown in Fig. 2.

$$\chi^2/\text{dof} = 1500/34 \text{ [A]}, 140/34 \text{ [B]}, 140/34 \text{ [C]}, 590/34 \text{ [E]}, 230/34 \text{ [F]} \quad (30)$$

With such  $\chi^2$ 's it is unlikely that any of the time-like pion form factor fits are truly correct models of the  $\pi$ - $\pi$  phase shift data, though the employed data sets are themselves not always consistent within  $1\sigma$ . Note, moreover, that points in the  $\rho$ - $\omega$  interference region have been included in the  $\chi^2$  computation, though in this region the  $\omega$  could influence the phase extracted from the  $\rho$  component of the form factor. Fit B is decidedly better than fit A; note that B differs from A only in that it incorporates the empirical scattering length. Fits C, E, and F are also similar in structure; they differ in the manner they parametrize the  $s$ -dependence of the form factor phase — fit C uses  $h(s)$ , Eqs. (10,9), whereas fits E and F use  $g(s)$ , Eqs. (18,17) — and in that the  $\rho'$  and  $\rho''$  contributions of fits E and F, Eq. (22) and Table IV, admit sources of phase beyond the  $\rho$ - $\omega$  sector. Fit C describes the  $\pi$ - $\pi$  phase shift slightly better than fits E and F. As fits C and D yield phase shifts of comparable shape — the  $\chi^2/\text{dof}$  for fit D is also 140/34 — it is the presence of the  $\rho'$  and  $\rho''$  contributions in fits E and F which is likely responsible for their poorer agreement with data. In particular, their inclusion increases the phase shift at large  $q$ . We have assumed that  $\delta_1^1$  is purely elastic in the regime shown, though the measured elasticity  $\eta_1^1$  does differ slightly from unity above 900 MeV [21]. The structure of fits E and F suggests that this assumption be examined. If the phase shift is not strictly elastic, that is, if  $\eta$  is not exactly unity, then the phase of the form factor  $\phi$  is related to the scattering phase shift  $\delta$  via [7]

$$\tan \phi \equiv \frac{\text{Im}F}{\text{Re}F} = \frac{(1 - \eta \cos 2\delta)}{\eta \sin 2\delta} . \quad (31)$$

If  $(1 - \eta) \ll 1$ , then  $\phi$  and  $\delta$  are related by

$$\phi = \delta + \frac{(1 - \eta) \cos \delta}{2\eta \sin \delta} \quad (32)$$

to leading order in  $(1 - \eta)$ . As  $\eta \leq 1$  and  $\delta_1^1 \gtrsim 100^\circ$  for  $q > 800$  MeV [21], Eq. (32) implies that  $\phi \leq \delta$  as well. Thus the structure of fits E and F would seem inconsistent with the manner in which they fit the phase shifts, for the phase of fits E and F exceeds that of C for  $s \gtrsim 900$  MeV, at odds with the constraint of Eq. (32). We conclude that the comparison

with the measured phase shifts indicates that fits B,C, and D would seem to be preferred. The average  $\rho$  parameters which emerge from these selected fits are  $m_\rho = 773$  MeV and  $\Gamma_\rho = 153$  MeV.

There is one last form factor constraint we can consider, for the pion form factor is known as  $s \rightarrow 0$  from chiral perturbation theory. Through two-loop order [38],

$$F_\pi(s) = 1 + \frac{1}{6} \langle r^2 \rangle_V^\pi s + c_V^\pi s^2 + f_V^U\left(\frac{s}{m_\pi^2}\right) + O(s^3), \quad (33)$$

where  $\langle r^2 \rangle_V^\pi$  is the electromagnetic charge radius of the pion squared and  $c_V^\pi$  is a low-energy constant. Note that  $f_V^U(\frac{s}{m_\pi^2})$  is the genuine loop contribution. A three-times-subtracted dispersion integral relates it to  $l = 1$ ,  $I = 1$   $\pi$ - $\pi$  scattering at the tree and one-loop level and to the pion form factor at the one-loop level [38]; a convenient analytic representation of  $f_V^U(\frac{s}{m_\pi^2})$  is given in Ref. [39].  $f_V^U(\frac{s}{m_\pi^2})$  possesses contributions at both  $O(s)$  and  $O(s^2)$ , yet the separation of the polynomial and dispersive pieces given in Eq. (33) suggests that its contribution to  $\langle r^2 \rangle_V^\pi$  is very small — indeed, this is numerically the case [38]. Crossing symmetry dictates the form of the  $O(s)$  term and thus offers a consistency check of the space-like and time-like region data.  $\langle r^2 \rangle_V^\pi$  has been measured in the space-like region by Amendolia *et al.*; adopting a fit in which  $|F_\pi(t)|^2 = n/(1 - t \cdot \frac{1}{6} \langle r^2 \rangle_V^\pi)^2$  and  $F_\pi(0) = n = 1.000 \pm 0.009$  yields  $\langle r^2 \rangle_V^\pi = 0.431 \pm 0.010 \text{ fm}^2$  [40]. The data of Amendolia *et al.* has been reanalyzed by Colangelo *et al.* using the form dictated by chiral perturbation theory, Eq. (33), and they find

$$\langle r^2 \rangle_V^\pi = 0.431 \pm 0.020 \pm 0.016 \text{ fm}^2 \quad (34)$$

$$c_V^\pi = 3.2 \pm 0.5 \pm 0.9 \text{ GeV}^{-4} \quad (35)$$

where the errors refer to statistical and theoretical uncertainties, respectively. The agreement of  $\langle r^2 \rangle_V^\pi$  with the value extracted by Amendolia *et al.* also indicates that the contribution of  $f_V^U(\frac{s}{m_\pi^2})$  at  $O(s)$  is small. The larger statistical error is a consequence of the two-parameter fit.

In the time-like region,  $\langle r^2 \rangle_V^\pi$  is determined by fits to data above the two-pion threshold,  $s \geq 4\pi^2$ . Ignoring the negligible  $\tilde{\Pi}_{\rho\omega}$  contribution, one has for fits A and B, *e.g.*, that

$$\langle r^2 \rangle_V^\pi = 6 \left( \beta_1 - \frac{1}{s_p} - \frac{1}{3} \left( \frac{3b\pi + 2}{c\pi - 2m_\pi^2} \right) \right), \quad (36)$$

whereas the  $\langle r^2 \rangle$  contribution from  $F_\rho^{\text{GS}}(s)$ , Eqs. (11,12,13), is

$$\langle r^2 \rangle = \frac{6}{m_\rho^2 + dm_\rho \Gamma_\rho} \left( 1 + \frac{1}{2\pi} \frac{\Gamma_\rho}{k_\rho} + \frac{\Gamma_\rho m_\rho}{2\pi k_\rho^2} \left( 1 + 2 \frac{m_\pi^2}{m_\rho^2} \right) \log \left( \frac{m_\rho + 2k_\rho}{2m_\pi} \right) - \frac{1}{3\pi} \frac{\Gamma_\rho m_\rho^2}{k_\rho^3} \right). \quad (37)$$

Using the parameters of Table II and IV, one finds

$$\langle r^2 \rangle_V^\pi (\text{fm}^2) = 0.30 \pm 0.04 \text{ [A]}, 0.35 \pm 0.03 \pm 0.02 \text{ [B]}, 0.36 \pm 0.03 \text{ [C\&D]}, 0.40 \pm 0.01 \text{ [E\&F]}. \quad (38)$$

Fit A does poorly on the  $a_1^1$  scattering length, so that its disagreement with the value of  $\langle r^2 \rangle_V^\pi$  from space-like data is not surprising. Fit B, however, is constrained to reproduce

$a_1^1$  and is much closer to the Colangelo *et al.* value [39]. Note that the errors associated with fit B are to be added in quadrature; the first error arises from the error in the fits, the second from the error in  $a_1^1$ . The agreement of fits C and D is comparable to that of fit B, whereas the results of fits E and F are within error of the Colangelo *et al.* value, when its error is taken into account as well. Thus, we see no real evidence for disagreement with the space-like data, and its consideration does not serve to distinguish the fits B–D, preferred by the phase shifts.

A plurality of conclusions exists in the literature concerning the consistency of the space-like and time-like data [15,41,42,25]. Of those who have argued that they are inconsistent [15,41], the difficulty seems to be with data at larger  $t$  [15,42], well beyond the region from which the charge radius is extracted.

Let us conclude this section by summarizing our results for the  $\rho$  mass and width. Fits A–D are all distinct in character and generate excellent fits to the time-like pion form factor data. Presuming that the central values are normally distributed, we can compute the variance of the central values to infer the theoretical systematic error in a particular parameter. Using the  $m$  prescription, so that the form factor is given by Eq. (6) as  $s \rightarrow m_\rho^2$ , averaging over the results of fits A–D yields,

$$m_\rho = 770.5 \pm 1.1 \pm 4.4 \text{ MeV} , \quad \Gamma_\rho = 153.5 \pm 0.9 \pm 4.0 \text{ MeV} , \quad (39)$$

where the errors reflect the experimental statistical and systematic uncertainties and the theoretical systematic uncertainties arising from the  $\rho$  parametrization chosen, respectively. Note that we have discarded the error arising from the use of the empirical scattering length in Fit B in the above, as realistically one would refit the parameters should the scattering length be varied. These values differ from those of Barkov *et al.*,  $m_\rho = 775.9 \pm 0.8 \pm 0.8$  MeV and  $\Gamma_\rho = 150.5 \pm 1.6 \pm 2.5$  MeV [12], though the most significant difference is in our respective estimates of the model errors, *cf.* 4.4 MeV with 0.8 MeV for the  $\rho$  mass and 4.0 MeV with 2.5 MeV for the  $\rho$  width. The theoretical systematic error we report is sensitive to the manner in which we determine the  $\rho$  mass and width. If, alternatively, we compute the mass and width from the value of the complex pole  $s_\rho$ , namely  $s_\rho \equiv \bar{m}^2 - i\bar{m}\bar{\Gamma}$ , we find for fits A–D that  $\bar{m}_\rho$  ranges from 756 to 757 MeV and  $\bar{\Gamma}_\rho$  ranges from 141 to 142 MeV. A similar parametrization insensitivity of the mass and width defined from the complex pole position has been noted in Ref. [6]. Note, however, for this latter choice, that the phase shift would not be  $\pi/2$  at  $s = \bar{m}_\rho^2$  and that the resultant form factor near  $s = \bar{m}_\rho^2$  would not be of Breit-Wigner form. Determining the mass and width as we have previously, but adopting the  $\tilde{m}$  prescription, noting Eq. (7), fits A–D yield

$$\tilde{m}_\rho = 774.3 \pm 1.1 \pm 4.4 \text{ MeV} , \quad \tilde{\Gamma}_\rho = 152.7 \pm 0.9 \pm 3.9 \text{ MeV} . \quad (40)$$

If we discard fit A for its poor fit to the  $\pi$ - $\pi$  phase shifts and repeat the above procedure for fits B–D only, we find

$$m_\rho = 773.0 \pm 0.7 \pm 1.2 \text{ MeV} , \quad \Gamma_\rho = 153.3 \pm 1.1 \pm 4.6 \text{ MeV} \quad (41)$$

and

$$\tilde{m}_\rho = 776.8 \pm 0.7 \pm 1.1 \text{ MeV} , \quad \tilde{\Gamma}_\rho = 152.6 \pm 1.1 \pm 4.5 \text{ MeV} . \quad (42)$$

This step-wise elimination procedure may not be reasonable, however, as slight adjustments of fit A may yield an acceptable simultaneous description of the  $l = 1$ ,  $I = 1$   $\pi$ - $\pi$  phase shift and time-like pion form factor data with comparable values of the  $\rho$  resonance parameters. We favor our determination based on the time-like form factor data alone, Eq. (39).

#### IV. CONCLUSIONS

We have determined the magnitude, phase, and  $s$ -dependence of the effective  $\rho$ - $\omega$  mixing matrix element  $\tilde{\Pi}_{\rho\omega}(s)$  from fits to  $e^+e^- \rightarrow \pi^+\pi^-$  data in the context of a theoretical framework which satisfies the analyticity, normalization, and phase constraints. We have considered a variety of descriptions which satisfy these theoretical constraints and have found the  $\rho$ - $\omega$  mixing parameters of interest to be insensitive to the manner in which the  $\rho$  is parametrized. Empirically  $\Gamma_\omega \ll \Gamma_\rho$ , and this likely drives the above result. Recalling Eqs. (23,24), we find

$$\begin{aligned}\tilde{\Pi}_{\rho\omega}(m_\omega^2) &= -3500 \pm 300 \text{ MeV}^2 \\ \tilde{\Pi}_{\rho\omega}^I(m_\omega^2) &= -300 \pm 300 \text{ MeV}^2 \\ \tilde{\Pi}'_{\rho\omega} &= 0.30 \pm 0.40 \text{ MeV}^2 ,\end{aligned}\tag{43}$$

where  $\tilde{\Pi}_{\rho\omega}^I(m_\omega^2)$  denotes the imaginary part of the effective mixing matrix element at  $s = m_\omega^2$  and  $\tilde{\Pi}'_{\rho\omega}$  characterizes the  $s$ -dependence of  $\tilde{\Pi}_{\rho\omega}(s)$  about  $s = m_\omega^2$ . Both the phase and  $s$ -dependence of  $\tilde{\Pi}_{\rho\omega}(s)$  are statistically insignificant. It is not that these effects are numerically trivial, but rather that they are poorly constrained by current  $e^+e^- \rightarrow \pi^+\pi^-$  data.

The value of  $\tilde{\Pi}_{\rho\omega}(m_\omega^2)$  we extract differs slightly from that extracted from the  $\omega \rightarrow 2\pi$  branching ratio, Eq. (29), that is,  $|\tilde{\Pi}_{\rho\omega}(m_\omega^2)| \approx 3900 - 4000 \text{ MeV}^2$ .  $\Gamma(\omega \rightarrow 2\pi)$  is itself extracted from the time-like pion form factor data, and its connection to  $\tilde{\Pi}_{\rho\omega}(m_\omega^2)$  explicitly involves the  $\rho$  parameters, which are relatively uncertain. It thus seems more appropriate to extract  $\tilde{\Pi}_{\rho\omega}(m_\omega^2)$  directly from  $e^+e^-$  data, as we have done. Were we to use Eq. (29) to extract  $B(\omega \rightarrow 2\pi)$  from our value of  $\tilde{\Pi}_{\rho\omega}(m_\omega^2)$ , not only would it be smaller than that which Barkov *et al.* reports [12], but it would also be explicitly sensitive to the  $\rho$  parametrization.

We have also systematically explored the  $\rho$  parameters associated with our parametrizations of the pion form factor. We find that the time-like data supports a range of  $\rho$  parameters. Adopting the prescription currently favored by the Particle Data Group [1], we find

$$m_\rho = 770.5 \pm 1.1 \pm 4.4 \text{ MeV} , \quad \Gamma_\rho = 153.5 \pm 0.9 \pm 4.0 \text{ MeV} ,\tag{44}$$

where the errors refers to the empirical and theoretical systematic uncertainties, respectively. It is worth noting that the differing prescriptions for the mass and width plague the direct comparison of the results of different groups, for the most recent world average for the  $\rho$  mass [1] mixes results defined under different conventions [43]. The convention favored by the Particle Data Group has itself changed with time, *cf.* the  $\tilde{m}$  convention, noting Eq. (7), of Ref. [47] with the  $m$  convention, noting Eq. (6), of Ref. [1], with no apparent adjustment of the reported values. We agree with the  $\rho$  width extracted by Barkov *et al.*,  $\Gamma_\rho = 150.5 \pm 1.6 \pm 2.5 \text{ MeV}$ , but their value for the  $\rho$  mass,  $m_\rho = 775.9 \pm 0.8 \pm 0.8 \text{ MeV}$ ,

seems slightly large [12]. It is the latter value that the Particle Data Group excludes on statistical grounds [1,14]. Note that our theoretical systematic errors are much larger than those reported by Barkov *et al.* [12], *cf.* 4.4 MeV with 0.8 MeV for the  $\rho$  mass. We have also studied the  $\rho$  parameters which result from different choices of data sets and find that the parameters extracted from the data of Barkov *et al.* are merely more precise. We conclude, then, that the data of Barkov *et al.* [16] are not likely wrong, but rather that the theoretical systematic errors associated with the extraction of the  $\rho$  parameters are larger than previously estimated.

### Acknowledgements

We thank W. Korsch for many discussions, much helpful advice, and for comments on the manuscript. We are grateful to C.B. Lang for promptly communicating the data included in the fits of Ref. [15] and to C.J. Horowitz and A.W. Thomas for helpful remarks. S.G. thanks U.-G. Meißner for suggesting the use of Ref. [38] and for helping us obtain the data of Hyams *et al.* [21], and H.O.C. thanks M. Benayoun and M.J. Peardon for helpful discussions. This work was supported by the U.S. Department of Energy under Grant DE-FG02-96ER40989.

## REFERENCES

- [1] Particle Data Group: R. M. Barnett *et al.*, Phys. Rev. D **54**, 1 (1996).
- [2] J. Pišút and M. Roos, Nucl. Phys. **B6**, 325 (1968).
- [3] M. Benayoun, Z. Phys. C **58**, 31 (1993).
- [4] K. Maltman, H. B. O’Connell, and A. G. Williams, Phys. Lett. B **376**, 19 (1996).
- [5] H. B. O’Connell, A. W. Thomas, and A. G. Williams, Nucl. Phys. **A623**, 559 (1997).
- [6] A. Bernicha, G. Lopez Castro, and J. Pestieau, Phys. Rev. D **50**, 4454 (1994).
- [7] B. Costa de Beauregard, B. Pire, and T. N. Truong, Phys. Rev. D **19**, 274 (1979). That  $\tilde{\Pi}_{\rho\omega}$  ought be real was first suggested by Ref. [8].
- [8] M. Gourdin, F. M. Renard, and L. Stodolsky, Phys. Lett. **30B**, 347 (1969); F. M. Renard,  $\rho - \omega$  Mixing, Springer Tracts in Modern Physics **63**, 98 (1972).
- [9] J. Gasser and H. Leutwyler, Phys. Rep. **87**, 77 (1982).
- [10] S. A. Coon and R. C. Barrett, Phys. Rev. C **36**, 97 (1987). See also S. A. Coon, M. D. Scadron, P. C. McNamee, Nucl. Phys. **A287**, 381 (1977).
- [11] H. B. O’Connell, B. C. Pearce, A. W. Thomas, and A. G. Williams, Phys. Lett. B **354**, 14 (1995).
- [12] L. M. Barkov *et al.*, Nucl. Phys. **B256**, 356 (1985).
- [13] Particle Data Group: L. Montanet *et al.*, Phys. Rev. D **50**, 1173 (1994).
- [14] M. Roos, private communication.
- [15] M. F. Heyn and C. B. Lang, Z. Phys. C **7**, 169 (1981).
- [16] OLYA detector: A. D. Bukin *et al.*, Phys. Lett. **73B**, 226 (1975); L. M. Kurdadze *et al.*, JETP Lett. **37**, 733 (1983); L. M. Kurdadze *et al.*, Sov. J. Nucl. Phys. **40**, 286 (1984); I. B. Vasserman *et al.*, Sov. J. Nucl. Phys. **30**, 519 (1979); CMD detector: G. V. Anikin *et al.*, Novosibirsk preprint INP 83-85 (1983). Note also S. R. Amendolia *et al.*, Phys. Lett. B **138**, 454 (1984); I. B. Vasserman *et al.*, Sov. J. Nucl. Phys. **33**, 368 (1981); L.M. Barkov *et al.*, Novosibirsk preprint INP 79-69 (1979); A. Quenzer *et al.*, Phys. Lett. **76B**, 512 (1978); G. Cosme *et al.*, ORSAY preprint LAL-1287 (1976).
- [17] V. Auslender *et al.*, Sov. J. Nucl. Phys. **9**, 69 (1969); V. Balakin *et al.*, Phys. Lett. **41B**, 205 (1972); D. Benaksas *et al.*, Phys. Lett. **39B**, 289 (1972); D. Bollini *et al.*, Nuovo Cim. **14**, 418 (1975); G. Cosme *et al.*, Phys. Lett. **63B**, 349 (1976); A. Bukin *et al.*, Phys. Lett. **73B**, 226 (1978); B. Esposito *et al.*, Phys. Lett. **67B**, 239 (1976); A. Quenzer *et al.*, Phys. Lett. **76B**, 512 (1978).
- [18] M. Lévy, Nuovo Cimento **13**, 115 (1959). See also R. E. Peierls, Proceedings of the 1954 Glasgow Conf. on Nuclear and Meson Physics, edited by E. H. Bellamy and R. G. Moorhouse (Pergamon, New York, 1955) p. 296.
- [19] R. G. Stuart, Phys. Rev. D **52**, 1655 (1995) and references therein.
- [20] P. Federbush, M. L. Goldberger and S. B. Treiman, Phys. Rev. **112**, 642 (1958).
- [21] B. Hyams *et al.*, Nucl. Phys. **B64**, 134 (1973) (W. Ochs, Thesis, University of Munich, 1974, unpublished); S. Protopescu *et al.*, Phys. Rev. D **7**, 1279 (1973).
- [22] S. Gasiorowicz, Elementary Particle Physics (John Wiley & Sons, New York, 1966).
- [23] K. M. Watson, Phys. Rev. **95**, 228 (1955).
- [24] G. J. Gounaris and J. J. Sakurai, Phys. Rev. Lett. **21**, 244 (1968).
- [25] B. V. Geshkenbein, Z. Phys. C **45**, 351 (1989).
- [26] G. F. Chew and S. Mandelstam, Phys. Rev. **119**, 467 (1960).
- [27] C.B. Lang and A. Mas-Parareda, Phys. Rev. D **19**, 956 (1979).

- [28] N. I. Muskhelishvili, Tr. Tbilisi Mat. Inst. **10**, 1 (1958); in *Singular Integral Equations*, edited by J. Radox (Noordhoff, Groningen, The Netherlands, 1953); R. Omnès, Nuovo Cimento **8**, 316 (1958).
- [29] B. W. Lee and M. T. Vaughn, Phys. Rev. Lett. **4**, 578 (1960).
- [30] M. Herrmann, B. L. Friman, and W. Nörenberg, Nucl. Phys. **A560**, 411 (1993).
- [31] F. Klingl, N. Kaiser, and W. Weise, Z. Phys. A **356**, 193 (1996).
- [32] C. B. Lang and I.-S. Stefanescu, Phys. Lett. **58B**, 450 (1975).
- [33] L. Castillejo, R. H. Dalitz, and F. J. Dyson, Phys. Rev. **101**, 453 (1956).
- [34] M. Nagels *et al.*, Nucl. Phys. **B147**, 189 (1979); O. Dumbrajs *et al.*, Nucl. Phys. **B216**, 277 (1983).
- [35] F. James and M. Roos, Comp. Phys. Comm. **10**, 343 (1975). See also [http://wwwinfo.cern.ch/asdoc/minuit\\_html3/minmain.html](http://wwwinfo.cern.ch/asdoc/minuit_html3/minmain.html) for the current version of the CERN Program Library long write-up D506, MINUIT.
- [36] P. R. Bevington and D. K. Robinson, Data Reduction and Error Analysis for the Physical Sciences, 2<sup>nd</sup> ed. (McGraw-Hill, New York, 1992).
- [37] Using the Barkov  $\omega \rightarrow 2\pi$  branching ratio and Particle Data Group values for the  $\rho$  and  $\omega$  parameters yields  $-3940 \text{ MeV}^2$ .
- [38] J. Gasser and U.-G. Meißner, Nucl. Phys. **B357**, 90 (1991).
- [39] G. Colangelo, M. Finkemeier, and R. Urech, Phys. Rev. D **54**, 4403 (1996).
- [40] S. R. Amendolia *et al.*, NA7 Collaboration, Nucl. Phys. **B277**, 168 (1986).
- [41] J. A. Alonso and J. A. Casas, Phys. Lett. B **197**, 239 (1987).
- [42] S. Dubnička and L. Martinovič, J. Phys. G **15**, 1349 (1989).
- [43] Note, for example, that Refs. [44,45] adopt the  $m$  prescription, so that the form factor is given by Eq. (6) as  $s \rightarrow m_p^2$ , whereas Refs. [15,46] adopt the  $\tilde{m}$  prescription, noting Eq. (7).
- [44] P. Weidenauer *et al.*, Z. Phys. C **59**, 387 (1993).
- [45] M. Aguilar-Benitez *et al.*, Z. Phys. C **50**, 405 (1991).
- [46] J. Bohacik and H. Kühnelt, Phys. Rev. D **21**, 1342 (1980).
- [47] Particle Data Group: C. Bricman *et al.*, Phys. Lett. **75B**, 1 (1978).



# TABLES

TABLE I. Components of  $F_\pi(s)$  for each fit. Note that “—” means  $\tilde{\Pi}_{\rho\omega}(s) = \tilde{\Pi}_{\rho\omega}(m_\omega^2)$ .

Fit	$\Omega(s)$	$F_{\text{red}}$	$\tilde{\Pi}_{\rho\omega}(s)$
A	Eq. (16)	Eq. (15)	—
A'	Eq. (16)	Eq. (15)	Eq. (24)
A <sup>I</sup>	Eq. (16)	Eq. (15)	Eq. (23)
B	Eq. (16) ( $c$ fixed)	Eq. (15)	—
C	Eq. (21)	Eq. (15)	—
D	Eq. (11)	Eq. (15)	—

TABLE II. Results from fitting the data of the Barkov *et al.* compilation from threshold through 923 MeV with  $F_\pi(s)$  as per Eq. (20) and Table I. Note that  $m_\pi = 0.13957$  GeV. In fit B, the first set of errors associated with the  $\rho$  resonance parameters is determined by the statistical and experimental systematic errors in the time-like pion form factor data, whereas the second set of errors arises from the error in the input empirical scattering length. \*Not a fitting parameter. †Input.

Parameter	A	B	C	A'	A <sup>I</sup>
$10^2 \cdot a \ (m_\pi^{-2})$	$-2.80 \pm 0.88$	$-0.672 \pm 0.084$	—	$-2.68 \pm 0.95$	$-2.57 \pm 1.06$
$b$	$0.24 \pm 0.52$	$-1.008 \pm 0.027$	$-1.403 \pm 0.023$	$0.17 \pm 0.56$	$0.10 \pm 0.63$
$c \ (m_\pi^2)$	$11.4 \pm 8.1$	30.45*	$36.48 \pm 0.66$	$12.5 \pm 8.7$	$13.7 \pm 9.6$
$\beta_1 \ (\text{GeV}^{-2})$	$-0.65 \pm 0.25$	$-0.27 \pm 0.12$	$-0.16 \pm 0.12$	$-0.69 \pm 0.25$	$-0.57 \pm 0.27$
$\beta_2 \ (\text{GeV}^{-4})$	$1.80 \pm 0.91$	$0.76 \pm 0.46$	$0.65 \pm 0.48$	$1.85 \pm 0.88$	$1.53 \pm 0.93$
$\beta_3 \ (\text{GeV}^{-6})$	$-0.97 \pm 0.68$	$-0.34 \pm 0.40$	$-0.29 \pm 0.42$	$-1.01 \pm 0.66$	$-0.79 \pm 0.68$
$\tilde{\Pi}_{\rho\omega} \ (\text{MeV}^2)$	$-3460 \pm 290$	$-3460 \pm 290$	$-3460 \pm 290$	$-3500 \pm 300$	$-3480 \pm 280$
$\tilde{\Pi}'_{\rho\omega}$	—	—	—	$0.027 \pm 0.040$	—
$\text{Im } \tilde{\Pi}_{\rho\omega} \ (\text{MeV}^2)$	—	—	—	—	$-310 \pm 280$
$\chi^2/\text{dof}$	68/75	68/76	68/76	67/74	66/74
Output					
$\tilde{s}_p \ (m_\pi^2)$	-12.46	-125.7	—	-14.21	-8.214
$a_1^1 \ (m_\pi^{-3})$	$0.084 \pm 0.043$	$0.038 \pm 0.002^\dagger$	$0.0324 \pm 0.0024$	$0.079 \pm 0.041$	$0.073 \pm 0.039$
$m_\rho \ (\text{MeV})$	$763.1 \pm 3.9$	$771.3 \pm 1.3 \pm 16$	$773.9 \pm 1.2$	$763.7 \pm 4.1$	$764.5 \pm 4.5$
$\Gamma_\rho \ (\text{MeV})$	$153.8 \pm 1.2$	$156.2 \pm 0.4 \pm 4.7$	$157.0 \pm 0.4$	$154.0 \pm 1.2$	$154.2 \pm 1.3$
$\tilde{m}_\rho \ (\text{MeV})$	$766.9 \pm 4.0$	$775.2 \pm 1.3 \pm 16$	$777.8 \pm 1.2$	$767.5 \pm 4.2$	$768.3 \pm 4.5$
$\tilde{\Gamma}_\rho \ (\text{MeV})$	$153.0 \pm 1.2$	$155.4 \pm 0.4 \pm 4.7$	$156.2 \pm 0.4$	$153.2 \pm 1.2$	$153.4 \pm 1.3$

TABLE III. More results from fitting the data of the Barkov *et al.* compilation from threshold through 923 MeV with  $F_\pi(s)$  as per Eq. (20) and Table I. Note that  $m_\pi = 0.13957$  GeV. Here the sensitivity of the  $s$ -dependence and phase of  $\tilde{\Pi}_{\rho\omega}(s)$  to the  $\rho$  parametrization is examined. \*Not a fitting parameter. <sup>†</sup>Input.

Parameter	B'	B <sup>I</sup>	C'	C <sup>I</sup>
$10^2 \cdot a \text{ (} m_\pi^{-2} \text{)}$	$-0.690 \pm 0.087$	$-0.712 \pm 0.090$	—	—
$b$	$-1.002 \pm 0.028$	$-0.993 \pm 0.030$	$-1.408 \pm 0.023$	$-1.413 \pm 0.024$
$c \text{ (} m_\pi^2 \text{)}$	$30.43 \pm 0.10^*$	$30.40 \pm 0.10^*$	$36.62 \pm 0.68$	$36.80 \pm 0.71$
$\beta_1 \text{ (GeV}^{-2} \text{)}$	$-0.35 \pm 0.15$	$-0.25 \pm 0.12$	$-0.25 \pm 0.16$	$-.14 \pm 0.13$
$\beta_2 \text{ (GeV}^{-4} \text{)}$	$0.93 \pm 0.49$	$0.68 \pm 0.46$	$0.82 \pm 0.51$	$0.56 \pm 0.48$
$\beta_3 \text{ (GeV}^{-6} \text{)}$	$-0.45 \pm 0.42$	$-0.28 \pm 0.40$	$-0.40 \pm 0.43$	$-0.22 \pm 0.42$
$\tilde{\Pi}_{\rho\omega} \text{ (MeV}^2 \text{)}$	$-3510 \pm 300$	$-3480 \pm 290$	$-3510 \pm 300$	$-3480 \pm 290$
$\tilde{\Pi}'_{\rho\omega}$	$0.034 \pm 0.039$	—	$0.035 \pm 0.039$	—
Im $\tilde{\Pi}_{\rho\omega} \text{ (MeV}^2 \text{)}$	—	$-340 \pm 270$	—	$-340 \pm 260$
$\chi^2/\text{dof}$	67/75	66/75	67/75	66/75
Output				
$\tilde{s}_p \text{ (} m_\pi^2 \text{)}$	-122.72	-119.01	—	—
$a_1^1 \text{ (} m_\pi^{-3} \text{)}$	$0.038 \pm 0.002^\dagger$	$0.038 \pm 0.002^\dagger$	$0.0323 \pm 0.0024$	$0.0321 \pm 0.0025$
$m_\rho \text{ (MeV)}$	$771.3 \pm 1.3 \pm 15$	$771.5 \pm 1.3 \pm 15$	$773.9 \pm 1.2$	$774.1 \pm 1.2$
$\Gamma_\rho \text{ (MeV)}$	$156.2 \pm 0.4 \pm 4.3$	$156.3 \pm 0.4 \pm 4$	$157.0 \pm 0.4$	$157.0 \pm 0.4$
$\tilde{m}_\rho \text{ (MeV)}$	$775.2 \pm 1.3 \pm 15$	$775.4 \pm 1.3 \pm 15$	$777.8 \pm 1.2$	$778.1 \pm 1.2$
$\tilde{\Gamma}_\rho \text{ (MeV)}$	$155.4 \pm 0.4 \pm 4.3$	$155.5 \pm 0.4 \pm 4$	$156.2 \pm 0.4$	$156.3 \pm 0.4$

TABLE IV. Results from fitting the data of the Barkov *et al.* compilation from threshold through 923 MeV with  $F_\pi(s)$  as per Eq. (22) and Eqs. (11,12,13). However, note that fit D, as per Table I, uses Eq. (20) with Eqs. (11,15) in place of Eq. (22). For Fit D  $\beta_1 = -0.16 \pm 0.12 \text{ GeV}^{-2}$ ,  $\beta_2 = 0.65 \pm 0.48 \text{ GeV}^{-4}$ , and  $\beta_3 = -0.29 \pm 0.42 \text{ GeV}^{-6}$ . The values of  $\tilde{\Pi}_{\rho\omega}(m_\omega^2)$  for fits E and F are determined from the fit to Eq. (22) via Eq. (25). \*Not a fitting parameter. †Input.

Parameter	D	E	F
$m_\rho$ (MeV)	$773.9 \pm 1.2$	$774.2 \pm 1.2$	$773.8 \pm 1.1$
$\Gamma_\rho$ (MeV)	$146.9 \pm 3.4$	$145.7 \pm 2.2$	$144.0 \pm 2.3$
$\alpha_\omega$	—	$(1.20 \pm 0.34) \cdot 10^{-3}$	$(1.50 \pm 0.28) \cdot 10^{-3}$
$\alpha_{\rho'}$	—	$1.01 \pm 0.18$	$0.467 \pm 0.096$
$\alpha_{\rho''}$	—	$-1.40 \pm 0.33$	$-0.70 \pm 0.20$
$m_{\rho'}$ (MeV)	—	$1465^\dagger$	$1290^\dagger$
$\Gamma_{\rho'}$ (MeV)	—	$310^\dagger$	$200^\dagger$
$m_{\rho''}$ (MeV)	—	$1700^\dagger$	$1590^\dagger$
$\Gamma_{\rho''}$ (MeV)	—	$235^\dagger$	$260^\dagger$
$\chi^2/\text{dof}$	68/76	74/77	71/77
$\tilde{\Pi}_{\rho\omega}$ (MeV <sup>2</sup> )	$-3460 \pm 290$	$-3610 \pm 310^*$	$-3580 \pm 310^*$
$\tilde{m}_\rho$ (MeV)	$777.3 \pm 1.2$	$777.6 \pm 1.2$	$777.1 \pm 1.1$
$\tilde{\Gamma}_\rho$ (MeV)	$146.2 \pm 3.3$	$145.1 \pm 2.2$	$143.4 \pm 2.2$
$a_1^1 (m_\pi^{-3})$	$(3.240 \pm 0.060) \cdot 10^{-2}$	$(3.208 \pm 0.036) \cdot 10^{-2}$	$(3.182 \pm 0.038) \cdot 10^{-2}$

TABLE V.  $\rho$  parameters and  $\tilde{\Pi}_{\rho\omega}(m_\omega^2)$  resulting from fits A–C of Table I and Eq. (20) to the time-like pion form factor data,  $|F_\pi(q^2)|^2$ . “40” denotes the 40 points of the 1978 world data. “60” denotes the OLYA and CMD data of Barkov *et al.*, whereas “82” denotes the data set compiled by Barkov *et al.*

Fit	$m_\rho$	$\Gamma_\rho$	$\tilde{\Pi}_{\rho\omega}$	$\chi^2/\text{dof}$
A40	$768 \pm 12$	$155.3 \pm 3.5$	$-2970 \pm 690$	41/33
A61	$759.7 \pm 4.1$	$152.8 \pm 1.2$	$-3340 \pm 300$	38/54
A82	$763.1 \pm 3.9$	$153.8 \pm 1.2$	$-3460 \pm 290$	68/75
B40	$769.7 \pm 3.6 \pm 15.5$	$155.7 \pm 1.1 \pm 4.5$	$-2970 \pm 690$	41/34
B61	$771.7 \pm 1.3 \pm 15.6$	$156.3 \pm 0.38 \pm 4.6$	$-3310 \pm 300$	43/55
B82	$771.3 \pm 1.3 \pm 16.1$	$156.2 \pm 0.37 \pm 4.7$	$-3460 \pm 290$	68/76
C40	$772.4 \pm 3.6$	$156.5 \pm 1.0$	$-2970 \pm 690$	41/34
C61	$774.0 \pm 1.2$	$157.2 \pm 0.4$	$-3310 \pm 300$	43/55
C82	$773.9 \pm 1.2$	$157.0 \pm 0.4$	$-3460 \pm 290$	68/76

# FIGURES

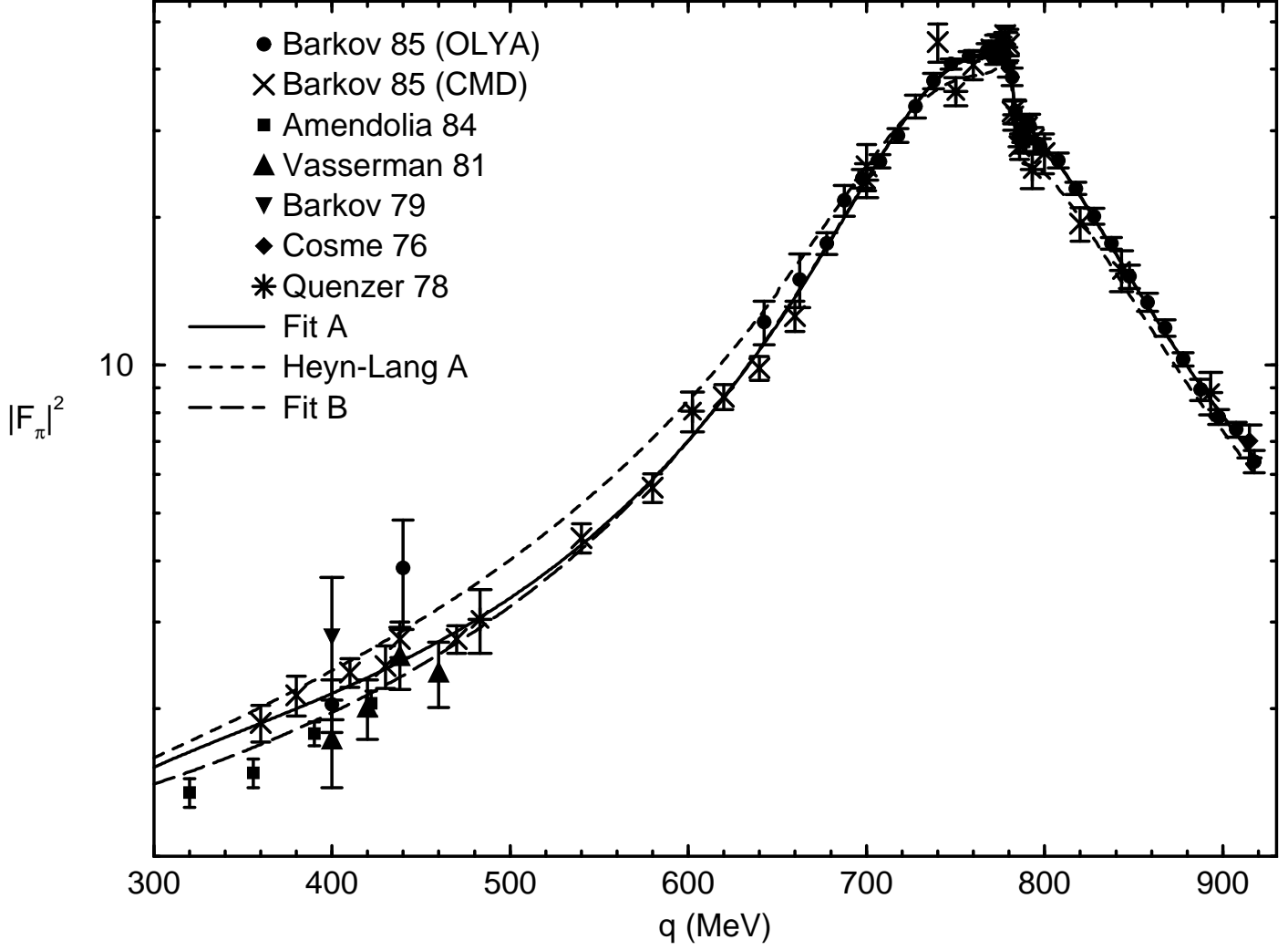


FIG. 1. The absolute square of the time-like pion form factor,  $|F_\pi(s)|^2$ , plotted versus the invariant mass  $q$  of the  $\pi^+\pi^-$  pair. Fits A (solid line) and B (long-dashed line), as per Eq. (20) and Table I, are shown with the data compiled by Barkov *et al.* The A fit, as per Table I, of Heyn and Lang (dashed line) is shown for reference.

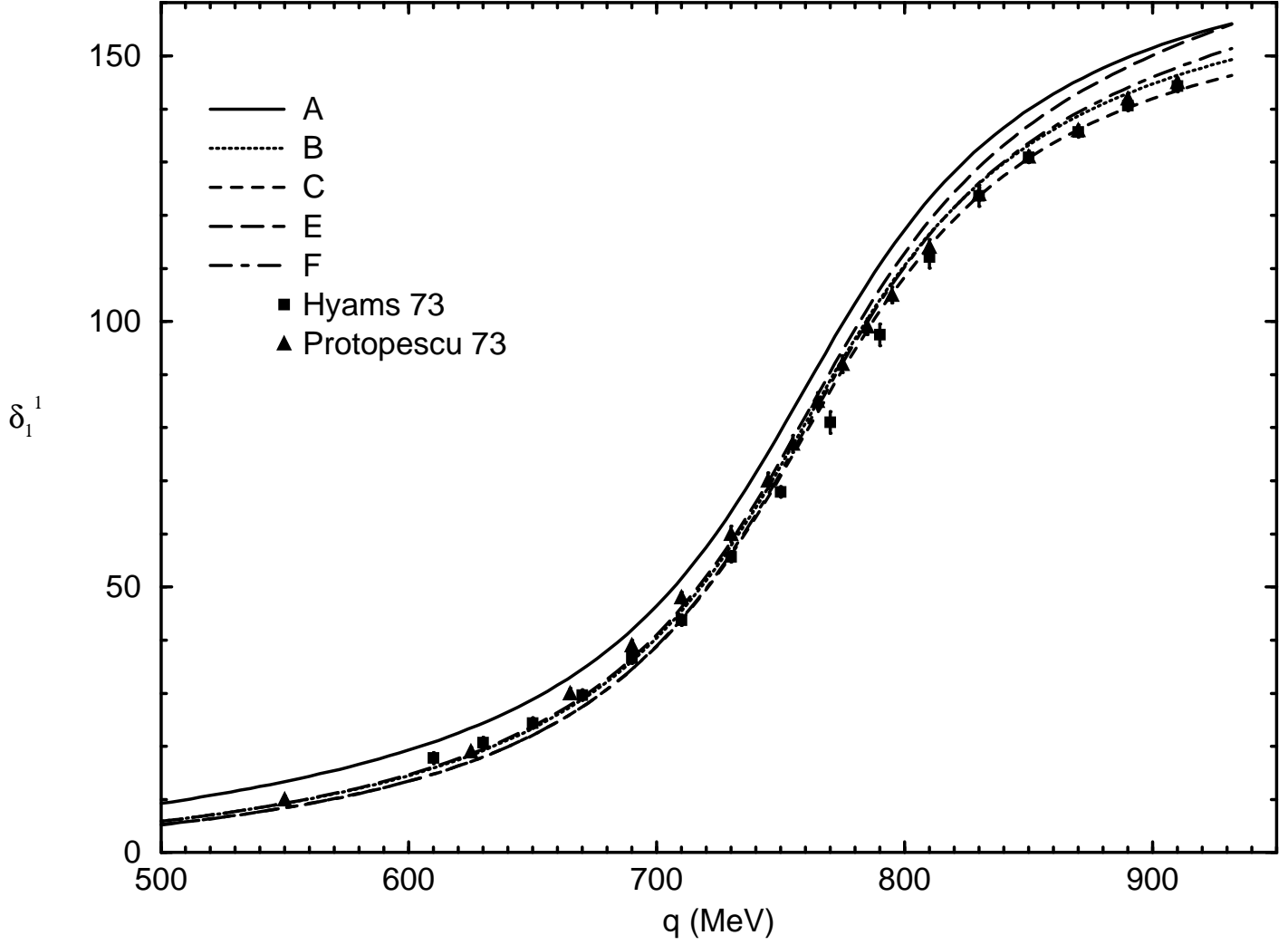


FIG. 2. The  $l = 1$ ,  $I = 1$   $\pi$ - $\pi$  phase shift  $\delta_1^1$  extracted from the phase of the time-like pion form factor as determined by fits A (solid line), B (dotted line), C (dashed line), E (long-dashed line), and F (dot-dashed line), given by Eqs. (20, 22) and Tables I, II, and IV, plotted versus the pion-pair invariant mass  $q$ , along with the data from Ref. [26]. Note that the  $\rho$ - $\omega$  mixing contribution to the time-like pion form factor phase has been omitted, to facilitate comparison with the empirical phase shifts.